Durham Research Online

A New Phase Field Model of a 'Gas of Circles' for Tree Crown Extraction from Aerial Images[*]

Peter Horváth[1,2] and Ian H. Jermyn[2]

[1] University of Szeged, Institute of Informatics, P.O. Box 652,
H-6701 Szeged, Hungary
Fax:+36 62 546 397
[2] Ariana (INRIA/I3S), INRIA,
B.P. 93, 06902 Sophia Antipolis, France
Fax:+33 4 92 38 76 43

Abstract. We describe a model for tree crown extraction from aerial images, a problem of great practical importance for the forestry industry. The novelty lies in the prior model of the region occupied by tree crowns in the image, which is a phase field version of the higher-order active contour inflection point 'gas of circles' model. The model combines the strengths of the inflection point model with those of the phase field framework: it removes the 'phantom circles' produced by the original 'gas of circles' model, while executing two orders of magnitude faster than the contour-based inflection point model. The model has many other areas of application *e.g.* , to imagery in nanotechnology, biology, and physics.

1 Introduction

Due to the high cost of field studies, forestry services are increasingly turning to image processing to gather the information they need. An important problem in this context is the extraction of the region in the domain of any given image corresponding to tree crowns. Using this information, forestry services can compute or estimate, for example, the mean diameter of the crowns, the biomass, and so forth. If tree crown extraction from aerial images could be performed automatically, then, in addition, expensive semi-automatic and manual image processing could be avoided.

In [1], we addressed this problem using 'higher-order active contours' (HOACs) [2], a new generation of active contours [3] allowing the incorporation of non-trivial prior knowledge about region geometry. Unlike most methods for incorporating prior geometric knowledge into active contours [4,5,6], HOACs do not necessarily constrain region topology, thereby allowing the detection of multiple instances of a single entity at no extra cost, a critical requirement for the current application.

To extract tree crowns, the HOAC model was analysed theoretically to find parameter values favouring regions composed of a number of approximate circles of approximately a given radius, by making such regions minima of the energy. The result was the 'gas of circles' model [1]. When combined with a likelihood energy, the model works

well, but suffers from some drawbacks: computation time is long, and the model can create 'phantom circles' in homogenous areas of the image. In [7], the parameters were further fixed so that circles are energy inflection points: they are not in themselves stable, but even a small amount of appropriate image information can render them stable. This removed the second drawback but not the first.

Rochery *et al.* [8] introduced an alternative formulation of HOACs, based on the 'phase field' framework used in physics. The basic phase field model is, to a good approximation, equivalent to a classical active contour, with energy given by boundary length. By adding a nonlocal term, phase field models equivalent to HOACs can be created. Phase fields have several advantages over other region modelling frameworks: a neutral initialization, obviating the need to choose an initial region; gradient descent based solely on the PDE arising from the model energy, thereby simplifying implementation, especially for HOACs; and enhanced topological freedom.

The purpose of the present paper is to construct the phase field version of the model of [7], thereby benefitting from all the advantages of the phase field framework, and solving both drawbacks of the model in [1]. In particular, we will see a gain of two orders of magnitude in execution time compared to the contour formulation.

In section 2, we give an overview of the original HOAC 'gas of circles' model. In section 3, we describe the phase field version. In section 3.2, we describe the phase field version of the HOAC inflection point 'gas of circles' model. In section 4 apply the model to the tree crown extraction problem, and we conclude in section 5.

2   Higher-Order Active Contours and the 'Gas of Circles' Model

HOACs can incorporate not only the local differential-geometric information included in classical active contours, but also more complex knowledge carried by long-range dependencies between tuples of contour points. These dependencies are expressed by multiple integrals over the contour. Combined with the classical region area and boundary length terms, one of the forms of Euclidean invariant quadratic HOAC energy is

$$E_{C,\mathrm{G}}(R) = \lambda_C L(\partial R) + \alpha_C A(\partial R) - \frac{\beta_C}{2} \iint dp\, dp'\, \dot{\gamma}(p) \cdot \dot{\gamma}(p') \Psi(r(p,p'),d) \ , \ (2.1)$$

where ∂R is the boundary of region R; γ is an embedding defining ∂R, and $\dot{\gamma}$ is its derivative; p is a coordinates on the domain of γ; L is the region boundary length functional; A is the region area functional; $r(p,p') = |\mathbf{r}(p,p')|$, where $\mathbf{r}(p,p') = \gamma(p) - \gamma(p')$; and Ψ is an interaction function, described in [1], parameterized by $d \in \mathbb{R}^+$, that determines the geometric content of the model.

2.1   The HOAC 'Gas of Circles' Model

For certain parameter ranges, circles, with radius r_0 depending on the parameters, are stable configurations of $E_{C,\mathrm{G}}$. These parameter ranges can be found by expanding $E_{C,\mathrm{G}}$ to second order in a functional Taylor series about a circle [1]. The series is most simply expressed in terms of the Fourier components of the perturbation: the first order term E_1 is zero for non-zero frequency $k \neq 0$, while the second order term E_2 is diagonalized by

the Fourier basis. Thus we require $E_1(r_0) = 0$ (energy extremum) and $E_2(k, r_0) > 0$ for all k (energy minimum). These two quantities are also functions of the model parameters λ_C, α_C, β_C, and d. The E_1 constraint determines β_C in terms of the other parameters, while the E_2 constraint restricts the range of α_C for given λ_C and d.

2.2   The HOAC Inflection Point 'Gas of Circles' Model

The above model has a disadvantage when minimized using gradient descent. Circles of the stable radius, once created, cannot disappear again because they are local minima, even if they have no support from the data. This problem was solved in [7], by further constraining the parameters so that the energy function has an inflection point at r_0 with respect to changes of radius (*i.e.* $E_2(0, r_0) = 0$), rather than a minimum. In this case, the effect of the data can easily create an energy minimum, but otherwise the circle will vanish. This second constraint fixes both α_C and β_C in terms of r_0, d, and λ_C. Since r_0 is fixed by the application, the only remaining parametric degrees of freedom are the value of d, and the overall strength of the prior term, represented by λ_C.

We also require α_C and β_C to be positive. When combined with the other constraints [7], this means that there is only a small range of permissible values of $\hat{r} = r_0/d$, to wit $0.6897 \le \hat{r} \le 0.7827$. This effectively enables d to be fixed, once r_0 is known. Thus despite the initial complexity of the model, we are able to fix all except one parameter, λ_C, representing the overall strength of the prior term.

3   Phase Fields and the 'Gas of Circles' Model

A phase field ϕ is a real-valued function on the image domain Ω. Given a threshold z, a phase field determines a region by the map $\zeta_z(\phi) = \{x \in \Omega : \phi(x) > z\}$. Thus phase fields are a level set representation. The difference with the usual distance function level set representation is that the functions are not constrained: the set of possible ϕ, Φ, is a linear space. The simplest phase field energy is

$$E_0(\phi) = \int_\Omega dx \left\{ \frac{D}{2} \partial\phi \cdot \partial\phi + \lambda(\frac{1}{4}\phi^4 - \frac{1}{2}\phi^2) + \alpha(\phi - \frac{1}{3}\phi^3) \right\} \ .$$

With $D = 0$, $\phi_R \triangleq \arg\min_{\phi:\ \zeta_z(\phi)=R} E_0(\phi)$, *i.e.* the minimizing phase field for a given fixed region, would take the value 1 inside R and -1 outside. The effect of $D \neq 0$ is to smooth ϕ_R so that it has an interface of finite width around ∂R. The phase field model is approximately[1] equivalent to a classical active contour in the sense that

$$E_0(\phi_R) \approx \lambda_C L(\partial R) + \alpha_C A(R) \triangleq E_{C,0} \ , \tag{3.1}$$

Equation (3.1) means that gradient descent on ϕ using E_0 will duplicate gradient descent on γ using $E_{C,0}$. The contour parameters are given by

$$\alpha_C = 4\alpha/3 \ , \quad \lambda_C^2 = 16D\lambda K/15 \ , \quad K = 1 + 5(\alpha/\lambda)^2 \ , \quad w^2 = 15D/\lambda K \ . \tag{3.2}$$

---

[1] For a detailed discussion of why the approximation error does not matter, see [8].

Rochery *et al.* [8] added the following nonlocal term to E_0:

$$E_{NL}(\phi) = -\frac{\beta}{2} \int_{\Omega^2} dx\, dx'\, \partial\phi(x) \cdot \partial\phi(x')\, G(x - x') \,, \qquad (3.3)$$

where $G(x - x') = \Psi(|x - x'|/d)$. With $\beta_C = 4\beta$, $E_g = E_0 + E_{NL}$ is equivalent (as usual, to a good approximation) to the HOAC model $E_{C,G}$, and can be used in its place, thus allowing the incorporation of non-trivial prior knowledge about region geometry while still profiting from all the advantages of the phase field framework.

3.1 The Phase Field 'Gas of Circles' Model

Using the relations between the phase field and contour parameters, we can now create a phase field 'gas of circles' model equivalent to the HOAC model described in section 2.1 (units are chosen so that $d = 1$):

1. Choose w. It cannot be too small, or a subpixel discretization will be needed, and it cannot be too large or the phase field model will not be a good approximation to the HOAC model [8]. We have found that $w = 3$ or $w = 4$ work well.
2. Choose $\tilde{\alpha}_C \leq \sqrt{5}/(2w)$. This constraint arises from inverting equations (3.2).
3. Determine the $\tilde{\beta}_C$ parameter corresponding to r_0 and $\tilde{\alpha}_C$ using the method in [1].
4. Set $\tilde{\lambda} = \frac{15}{8w}[1 + \sqrt{1 - 4\tilde{\alpha}_C^2 w^2/5}]$, $\tilde{\alpha} = 3\tilde{\alpha}_C/4$, $\tilde{\beta} = \tilde{\beta}_C/4$, and $\tilde{D} = w/4$.
5. Choose λ_C and multiply $\tilde{D}$, $\tilde{\lambda}$, $\tilde{\alpha}$, and $\tilde{\beta}$ by it to get D, λ, α, and β.

3.2 The Phase Field Inflection Point 'Gas of Circles' Model

We now want to combine the phase field 'gas of circles' model with the constraint that the circle energy have an inflection point rather than a minimum at the desired radius. This is a non-trivial requirement. The relations between the phase field and contour parameters were derived using an approximate ansatz for ϕ_R [8]. For the 'gas of circles' model, the approximations are not expected to be important, since small errors in the parameters will produce small changes in behaviour. However, an inflection point represents a set of measure zero in the parameter space. It is important to see whether these approximate parameter relations preserve the inflection point behaviour.

In the previous section, we chose $\tilde{\alpha}_C$ according to the constraint $\tilde{\alpha}_C \leq \sqrt{5}/(2w)$. In section 2, we described how a given value of $\hat{r}$ fixes $\tilde{\alpha}_C$ and $\tilde{\beta}_C$. To satisfy both these constraints we need to choose $w \leq \sqrt{5}/2\tilde{\alpha}_C$. To determine the parameters of the new phase field inflection point 'gas of circles' model, we therefore take the following steps:

1. Choose an $\hat{r}$ value satisfying $0.6897 \leq \hat{r} \leq 0.7827$. This fixes $\tilde{\alpha}_C$ and $\tilde{\beta}_C$.
2. Choose w using the above criterion.
3. Determine $\tilde{\lambda}$, $\tilde{\alpha}$, $\tilde{\beta}$, and $\tilde{D}$ as before.
4. Multiply these parameters by λ_C.

To test that the parameter transformations work in practice, we fixed a set of contour parameters corresponding to an inflection point at $r_0 = 10$, and then translated these parameters to give an equivalent phase field model. We then performed three gradient descent experiments using E_g. One used the value of β corresponding to the inflection
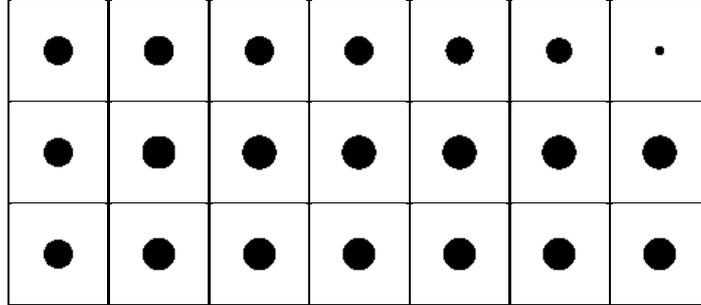
Fig. 1. Preservation of the inflection point when translating from contour to phase field: gradient descent evolutions using E_g, starting from a circle of radius $r_0 = 10$, for values of β close to β^*, the value giving an inflection point at $r_0 = 10$. Row 1: evolution using $\beta_C = 0.96\beta^*$; row 2: evolution using $\beta = 1.04\beta^*$; row 3: evolution using $\beta = \beta^*$.

point, β^*, while the other two used β values 4% above and below β^*. The region was initialized to a circle of radius r_0. Figure 1 shows the results. In the first row, with $\beta < \beta^*$, the region shrinks and disappears. In the second row, with $\beta > \beta^*$, the region grows until it reaches the corresponding energy minimum, at a radius of 12 pixels. In the third row, with $\beta = \beta^*$, the circle grows only very slightly, to a radius of 10.5 pixels. The inflection point behaviour is therefore preserved to a very good approximation.

4   Tree Crown Extraction

The tree crown extraction problem has been studied in several papers. Gougeon [9] uses a valley following method to delineate the crowns, while Larsen [10] introduces a species-specific method based on the matching of 3D tree templates. Both these, and other similar methods, look for local maxima of certain features. Perrin *et al.* [11] use a global method, modelling tree crown configurations as a marked point process. This has the advantage over our method that overlapping trees are easily handled, but the disadvantage that trees are represented by ellipses: their outlines are not found.

Our model for tree crown extraction is the sum of two terms: a prior energy E_g, as described above, and a likelihood energy, E_i, which we will now describe. We will model the image I, both in R and in the background $\bar{R}$, using Gaussian distributions.[2] We add a term that predicts high gradients along the boundary ∂R:

$$E_i(I, R) = \int_\Omega dx \left\{ \lambda_i \, \partial I \cdot \partial \phi + \alpha_i \left[\frac{(I - \mu)^2}{2\sigma^2} \phi_+ + \frac{(I - \bar{\mu})^2}{2\bar{\sigma}^2} \phi_- \right] \right\},$$

where $\phi_\pm = (1 \pm \phi)/2$. Note that to facilitate comparison of parameters in the prior energy, we set $\lambda = 1$ in E_g and introduce a weight α_i in E_i.

---

[2] We ignore the normalization constant $Z(R) = \int DI \, e^{-E_i(I,R)}$ since in our case it merely changes λ and α, and we are interested in stability of the posterior in the absence of image-dependent terms.
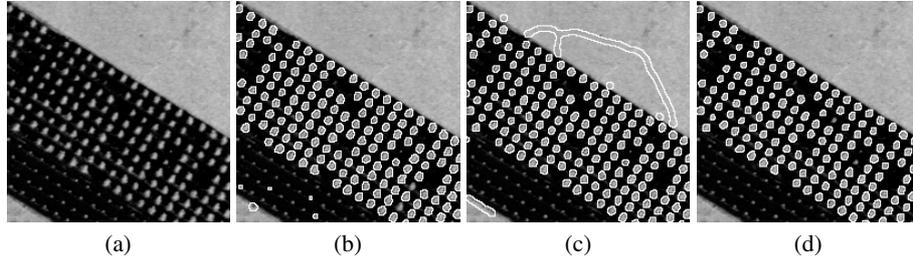
| (a) | (b) | (c) | (d) |

Fig. 2. (a) an image of poplars © IFN (0.6, 0.06, 0.33, 0.19, 2.5); (b) the result with the HOAC 'gas of circles' model with inflection point (1160, 0.7); (c) result with the phase field 'gas of circles' model (1111, 278, 177.2, 55.8, 30, 4); (d): result with the new model (1160, 0.7, 4)

4.1 Energy Minimization

We minimize $E = E_g + E_i$ using gradient descent. The functional derivative of E_{NL} is

$$\frac{\delta E_{NL}}{\delta \phi}(x) = \beta \int_{\Omega} dx'\, \partial^2 G(x - x')\phi(x') \,. \tag{4.1}$$

The nonlocal force arising from the HOAC term makes gradient descent using $E_{C,G}$ complex to implement. One must extract the contour, perform numerical contour integrations, and extend the force off-contour [2]. In contrast, the force (4.1) arising from the nonlocal phase field term is simply a convolution. Implementation is thereby made much simpler, and execution much faster. The time for one iteration in the HOAC formulation scales as the square of the boundary length, which scales as the number of trees, which in turn scales as the number of pixels. Thus execution time for the HOAC formulation can be expected to scale as the number of pixels squared. In contrast, execution time for the phase field formulation scales linearly with the number of pixels.

4.2 Experimental Results

Our data are $\sim$ 0.5m resolution colour infrared aerial images of the 'Saône et Loire' region in France provided by the French National Forest Inventory. The images show regularly and irregularly planted poplar forests.

We compared the new phase field inflection point 'gas of circles' model (section 3.2) with the HOAC inflection point 'gas of circles' model (section 2.2) and with the phase field 'gas of circles' model with a minimum rather than an inflection point (section 3.1). The parameters μ, σ, $\bar{\mu}$, and $\bar{\sigma}$ are learned from examples using maximum likelihood, and then fixed. [3]

Figure 4.1(a) shows an image (200 × 200) of a regularly planted poplar forest. In the top right and bottom left there are fields, while in the middle, two different sizes of poplars. The aim is to extract the larger trees. Figure 4.1(b) shows the result with the

---

[3] In the figure captions, the image parameters are (μ, σ, $\bar{\mu}$, $\bar{\sigma}$, r_0); in the HOAC 'gas of circles' case, the prior parameters are (α_i, $\hat{r}$), in the phase field 'gas of circles' case they are (α_i, D, λ, α, β, w); while in the case of the new model they are (α_i, $\hat{r}$, w).
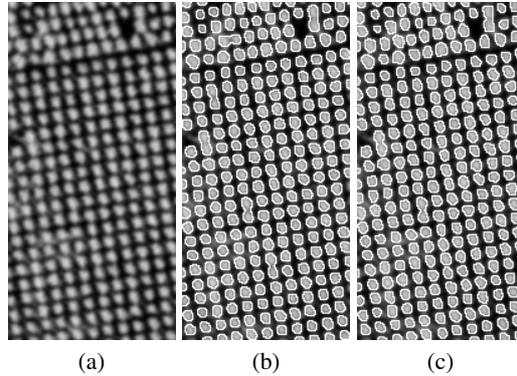
Fig. 3. (a) An image of regularly planted poplar stands with a less regularly planted trees at the upper part © IFN (0.8, 0.06, 0.43, 0.2, 3.5); (b) result with the phase field 'gas of circles' model (500, 50, 34.2, 9.3, 5.2); (c) result with the new model (500, 0.74, 4)
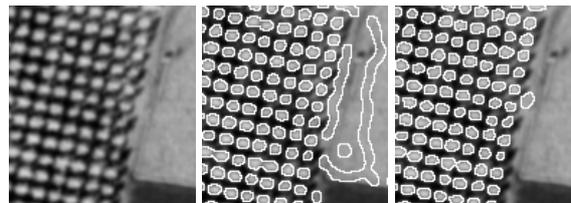

Fig. 4. (a) An image of regularly planted poplars with different fields in the right part © IFN (0.8, 0.06, 0.43, 0.2, 3.5); (b) result with the phase field 'gas of circles' model (500, 50, 34.2, 9.3, 5.2); (c) result with the new model (500, 0.74, 4)

HOAC inflection point 'gas of circles' model. The result is good, but the method found two small trees, and there is another false positive in the bottom left of the image. The execution time was 89 minutes. Figure 4.1(c) shows the result using the phase field 'gas of circles' model. There were no false negatives, but the model found false positives in the fields. Figure 4.1(d) shows the result with the new phase field inflection point 'gas of circles' model. All but two somewhat smaller circles were successfully found. For the phase field models, the execution time was less than 3 minutes.

Figure 4.2(a) shows an image (133 × 271) of a planted forest. Figure 4.2(b) shows the result with the phase field 'gas of circles' model. The result is good, with only a few joined tree crowns. Figure 4.2(c) shows the result with the new model. There are fewer joined tree crowns. Both results were obtained in less than 2 minutes.

Figure 4.2(a) shows a difficult image (129 × 139) to analyse. It has two fields with different intensities on the right. The result with the phase field 'gas of circles' model is shown in figure 4.2(b). This result clearly demonstrate the disadvantage of the non-inflection point model: phantom objects are created in the homogenous areas. Figure 4.2(c) shows the result with the new model. The result is very good, with only one false positive. Both results were obtained in less than 1 minute.

5   Conclusion

We have described a phase field version of the HOAC inflection point 'gas of circles' model described in [7]. The model was applied to the problem of tree crown extraction from aerial images, a problem of great practical importance for the forestry industry. The model combines the strengths of the inflection point model with those of the phase field framework: it removes the 'phantom circles' produced by the original 'gas of circles' model, while executing two orders of magnitude faster than the contour model.

References

1. Horváth, P., Jermyn, I.H., Kato, Z., Zerubia, J.: A higher-order active contour model for tree detection. In: Proc. International Conference on Pattern Recognition (ICPR), Hong Kong, China (2006)
2. Rochery, M., Jermyn, I.H., Zerubia, J.: Higher-order active contours. International Journal of Computer Vision 69, 27–42 (2006)
3. Kass, M., Witkin, A., Terzopoulos, D.: Snakes: Active contour models. International Journal of Computer Vision 1, 321–331 (1988)
4. Cremers, D., Kohlberger, T., Schnörr, C.: Shape statistics in kernel space for variational image segmentation. Pattern Recognition 36, 1929–1943 (2003)
5. Foulonneau, A., Charbonnier, P., Heitz, F.: Geometric shape priors for region-based active contours. In: Proc. IEEE International Conference on Image Processing (ICIP). vol. 3, pp. 413–416 (2003)
6. Leventon, M., Grimson, W., Faugeras, O.: Statistical shape influence in geodesic active contours. In: Proc. IEEE Computer Vision and Pattern Recognition (CVPR), Hilton Head Island, SC, USA, pp. 316–322 (2000)
7. Horváth, P., Jermyn, I.H., Kato, Z., Zerubia, J.: An improved 'gas of circles' higher-order active contour model and its application to tree crown extraction. In: Kalra, P., Peleg, S. (eds.) ICVGIP 2006. LNCS, vol. 4338, Springer, Heidelberg (2006)
8. Rochery, M., Jermyn, I., Zerubia, J.: Phase field models and higher-order active contours. In: Proc. IEEE International Conference on Computer Vision (ICCV), Beijing, China (2005)
9. Gougeon, F.A.: Automatic individual tree crown delineation using a valley-following algorithm and rule-based system. In: Hill, D., Leckie, D. (eds.) Proc. International Forum on Automated Interpretation of High Spatial Resolution Digital Imagery for Forestry, Victoria, British Columbia, Canada, pp. 11–23 (1998)
10. Larsen, M.: Finding an optimal match window for Spruce top detection based on an optical tree model. In: Hill, D., Leckie, D. (eds.) In: Proc. International Forum on Automated Interpretation of High Spatial Resolution Digital Imagery for Forestry, Victoria, British Columbia, Canada, pp. 55–66 (1998)
11. Perrin, G., Descombes, X., Zerubia, J.: A marked point process model for tree crown extraction in plantations. In: Proc. IEEE International Conference on Image Processing (ICIP), Genova, Italy (2005)